Powder Technology 285 (2015) 51–61

Contents lists available at ScienceDirect

Powder Technology

journal homepage: www.elsevier.com/locate/powtec

Polymeric microparticles containing indomethacin for inhalatory administration

Nazareth Eliana Ceschan [a,b], Verónica Bucalá [a,b], María Verónica Ramírez-Rigo [a,c,*]

[a] Planta Piloto de Ingeniería Química (PLAPIQUI), CONICET — Universidad Nacional del Sur (UNS), Camino La Carrindanga Km 7, (8000) Bahía Blanca, Argentina
[b] Departamento de Ingeniería Química, UNS, Avenida Alem 1253, (8000) Bahía Blanca, Argentina
[c] Departamento de Biología, Bioquímica y Farmacia, UNS, San Juan 670, (8000) Bahía Blanca, Argentina

ARTICLE INFO

Available online 16 February 2015

Keywords:
Polyelectrolyte–drug complexes
Pulmonary route
Non-steroidal antiinflammatory drug
Spray drying
Polylysine
Particle engineering

ABSTRACT

Indomethacin (IN) is a non-steroidal antiinflammatory drug. It reduces pain and inflammation in rheumatoid arthritis but its use is associated with high incidence of undesirable gastrointestinal side effects. In addition, its low solubility in water limits its oral bioavailability. In this work, microparticles based on an IN–polylysine (PL) complex were obtained by spray drying. The system is intended to deliver the drug through the inhalatory route for both local and systemic treatments. Several formulations, varying the relative composition IN/PL–dextrin (DX) and the total solid content of the feed solutions, were tested. The process performance (yield, air outlet temperature), product properties (IN load efficiency, moisture content, crystallinity, glass transition temperature, density, morphology and particle size distribution), the IN–polylysine ionic interaction (assessed by FT-infrared spectroscopy, powder X-ray diffraction and thermal analysis), and in vitro IN release were studied. Powders exhibited high load efficiencies and low moisture contents, and remained in the amorphous state after nine months of storage. The particle systems with 50% of the polylysine amino groups neutralized by IN were the more attractive ones for pulmonary treatment, since they were easily processed using a homogeneous aqueous feed, had relatively high IN contents and high cumulative fraction of respirable particles.

1. Introduction

Non-steroidal antiinflammatory drugs (NSAIDs) are a family of active ingredients that shares pharmacological applications and side effects. In general, they have analgesic, antiinflammatory and antipyretic properties [1]. The World Health Organization developed a 3-step conceptual model to guide the pain management, suggesting that the NSAIDs should be the first option in chronic and acute therapies [2]. Common side effects of NSAIDs are gastrointestinal lesions, the most frequently ones are minor and well tolerated. However, the NSAIDs can also cause erosions and gastric and duodenal ulcers. Less often, NSAIDs cause kidney problems, hypersensitivity and hematologic reactions [1]. Due to gastrointestinal complications, NSAIDs are the second pharmacological group more recurrently involved in adverse reactions to drugs. From the all side effects treated in hospitals, 20% are because of NSAIDs. Between 1 and 3% of people who consume these medicines for at least one year develop adverse drug reactions, and 5–10% of them suffer gastric ulcers [3].

Inhalatory route is an attractive non-invasive alternative route for the delivery of active ingredients in local and systemic treatments [4]. Currently the global market for this type of drug delivery is growing rapidly. Both nasal and pulmonary administration allows improving bioavailability, because an extensive surface area and an epithelial layer highly vascularized are available for absorption. Also, the inhalatory administration allows avoiding the hepatic first-pass metabolism [4]. Particularly, inhalatory route is an interesting alternative for gastrolesive active ingredients like NSAIDs. Within this drug group, nasal and pulmonary administration of ketoprofen, meloxicam and ibuprofen was previously addressed [5–7]. The developed formulations (aerosols and dry powders) were designed to avoid the oral administration of NSAIDs and to treat local illnesses of the upper respiratory tract.

Other drug candidate for inhalatory administration is Indomethacin (IN), a NSAID derived from indoleacetic acid (Fig. 1a). It reduces pain and inflammation in osteoarthritis, rheumatoid arthritis and tendinitis [8]. Although it is a very effective drug, it presents low oral bioavailability due to its poor aqueous solubility [8] when it is administered as immediate release solid oral dosage forms. According to the Biopharmaceutics Classification System, IN is categorized as class II drug (low solubility and high oral permeability [8]). Consequently, important efforts were done to improve IN dissolution rate for oral applications. Among others, particle size reduction, usage of IN at its amorphous state and preparation

* Corresponding author at: Planta Piloto de Ingeniería Química (PLAPIQUI), CONICET — Universidad Nacional del Sur (UNS), Camino La Carrindanga Km 7, (8000) Bahía Blanca, Argentina. Tel.: +54 291 486 1700x265; fax: +54 291 486 1600.
E-mail address: vrrigo@plapiqui.edu.ar (M.V. Ramírez-Rigo).

http://dx.doi.org/10.1016/j.powtec.2015.02.001
0032-5910/

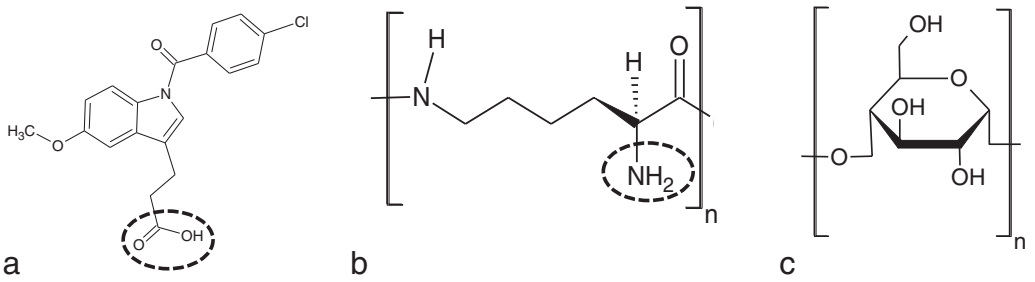

Fig. 1. Structural formula of a) indomethacin (IN) b) polylysine (PL) and c) dextrin (DX, only the α 1, 4 link is represented). Circles highlight the acidic and basic groups of IN and PL that participate in the complex formation, respectively.

of aqueous soluble inclusion complexes carrying the drug [9,10]. In particular, the amorphous state of IN was extensively studied; however this state is unstable, limiting its application [10]. Regarding the IN particle size reduction, it was reported a size limit for which further size reduction did not improve the dissolution rate and moreover particle agglomeration can be observed [11]. Inclusion complexes have the disadvantages of a limited drug load efficiency [9].

Moreover, its use is limited because of the high incidence of gastrointestinal side effects [1,8]. The IN inhibits the secretion of prostaglandins that protect gastric tissues and has relative large residence times in contact with the stomach mucosa because at acid pH this drug is trapped and accumulated within cells [1]. The most frequently gastrointestinal complications are dyspepsia, hyperacidity, nausea, vomiting and epigastric pain, ulcers and erosions [1]. For this reason, alternative systemic administration routes were explored to avoid the acute local pH-dependent [12,13]. Among them, the inhalatory route was explored. Huang et al. [14] studied in vivo the IN nasal administration delivered as a solution (with sodium bicarbonate) and demonstrated that IN has an adequate absorption through the nasal mucosa and can reach the systemic circulation in a similar way than when it is orally administered. Based on this result, Karasulu et al. [15] also studied in vivo the IN nasal administration using emulsions with different excipients to enhance the drug permeation and thus the bioavailability. Although these previous contributions are interesting, the IN pulmonary administration would allow both systemic and local treatments of patients with rheumatoid arthritis-associated lung disease [16]. In this sense, Onischuk et al. [17] explored the effectiveness of pulmonary administration of pure IN in mice proving that lower doses of IN are necessary to achieve the joint anti-inflammatory action compared to oral administration. However, the dose deposited in the lung is low.

To deliver this drug to the alveolus, it is necessary to design a formulation capable to reach the lung respiratory regions. The current tendency of inhalable systems is oriented to dry powder inhalers, which have competitive advantages in terms of stability and efficiency over nebulization systems or metered dose inhalers [18]. However, for dry powder inhalers a rational design of the particulate system is required. The characteristics of the material (shape, size, density, porosity, surface charge, chemical composition, among others) strongly affect the particles' aerosolization and deposition, as well as the drug release and residence time at the action or absorption site [19]. Therefore, the powder properties modify significantly the biopharmaceutical performance of the formulation [19].

Spray drying (SD) is a technology for producing particulate systems with controlled quality by a suitable selection of the fluid feed composition and process operating conditions [19]. This process is currently selected to develop inhalable particles because it is a scalable continuous technology, able to process a variety of liquid feeds (solutions, dispersions and emulsions) based on substances of different natures [19,20].

To overcome IN physicochemical and biopharmaceutical problems, an adequate formulation design of feed fluid is necessary to enhance the product properties. In this work the preparation of inhalable particulate systems based on ionic complexes between IN and a polyelectrolyte is proposed to improve the IN bioavailability and to avoid the gastrointestinal adverse side effects of this drug. For the inhalatory route, epsilon-polylysine (PL) is an interesting polyelectrolyte (polymer with amino groups in its structure; Fig. 1b) due to its high water solubility, biodegradability, non-toxicity [21] and because it was demonstrated to be biocompatible with pulmonary tissues ex vivo for genic therapy [22]. Considering that the polylysine can interact with anionic compounds, the combination PL–IN is postulated as a chemical entity with properties different from its precursors, as it was demonstrated for another polyelectrolyte–drug combinations [23].

Some reports related to inhalatory materials based on polyelectrolyte–drug complexes prepared by SD are available for hyaluronic acid [24], poly-epsilon-caprolactone [25], dextran [26] and alginic acid [20] combined with fluoroquinolones or atenolol. However the solid state properties of materials based on cationic polyelectrolytes and poorly water soluble drugs as well as the relationships between the process and the product quality are fields that still are required to be explored.

Therefore, the present study addressed the principles associated with the production of novel microparticles intended for pulmonary IN delivery for rheumatoid arthritis treatment. Varying the feed formulation (i.e. IN and PL/DX ratios), the powders were obtained by SD. The process performance (SD yield, air outlet temperature), product properties (IN load efficiency, moisture content, crystallinity, glass transition temperature, density, morphology and particle size distribution), the IN–PL ionic interaction (assessed by Fourier transform infrared spectroscopy, powder X-ray diffraction and thermal analysis), and IN release in vitro were extensively studied.

2. Materials and methods

2.1. Materials

Indomethacin (pharmaceutical grade, Parafarm, Saporiti, Buenos Aires, Argentina) was used as active pharmaceutical ingredient. In this work, epsilon-polylysine (food grade, Purac America, Lincolnshire, United States) was used as received from suppliers, i.e. as a mixture of polylysine:dextrin (PL:DX 50:50). Dextrin is a polysaccharide (α-1,4 poly(glucose) polymer that contains few, <5%, α-1,6 links displaying minimal branching; Fig. 1c) and, as other sugars like lactose and mannitol, allows improving flow properties [27] and storage stability [28]. This compound, which is highly water soluble, was previously used as biocompatible excipient in pulmonary product development [29]. Its association with polylysine was proposed to improve the PL conformational structure stability [28].

Lactose monohydrate (−70 + 140 ASTM Mesh, pharmaceutical grade, Parafarm, Saporiti, Buenos Aires, Argentina), potassium bromide (spectroscopic grade, Parafarm, Saporiti, Buenos Aires, Argentina), potassium phosphate monobasic (analytical grade, Anedra, Buenos Aires, Argentina), sodium hydroxide (analytical grade, Anedra, Buenos Aires, Argentina), size 3 gelatine capsules (pharmaceutical grade, Parafarm, Saporiti, Buenos Aires, Argentina) and distilled water were also used.

2.2. Determination of number of equivalents of amino groups in PL

The available PL amino groups were determined by direct potentiometric titration [30] using a HCl solution (0.009810 N). The PL raw material had 3.39×10^{-3} equivalents of amino groups per gram.

2.3. Solution preparation

To study the influence of the feed composition on the properties of powders obtained by spray drying, 200 mL of aqueous solutions containing different amounts of IN and PL:DX was prepared. As it can be seen in Table 1, the samples were named according to their theoretical composition as $(PL–IN)_x$:DX Y%, x refers to the neutralization degree of PL amino groups and Y to the theoretical total solid content of the solutions.

To assess the influence of PL:DX/IN ratio on the spray-dried powder, PL amino groups neutralization degrees of 25, 50 and 75% were selected. For these samples, a total solid content of 1.6% w/v was selected in order to evaluate the influence of the neutralization degree on product quality and process performance. This goal was achieved with $(PL–IN)_{25}$:DX 1.6% and $(PL–IN)_{50}$:DX 1.6% feed solutions. However, two phases were observed in the $(PL–IN)_{75}$:DX 1.6% fluid. Consequently only the supernatant of this sample was analyzed (Section 2.4.) and fed (Section 2.5.) to the SD, being the experimental total solid content of the supernatant 1.4%.

For comparative purposes, PL:DX 1.6% w/v solution was also processed by SD. Due to the low solubility in water (5 μg/mL at 25 °C [31]) and the instability of the IN–water dispersions, raw IN was not spray dried.

Also for a given neutralization degree (50%) and IN relative composition (0.3 $g_{IN}/g_{PL:DX}$) the total solid concentrations were varied: 0.6, 1.3, 1.6 and 2.6% w/v.

2.4. Characterization of the SD feed solutions

2.4.1. pH

The pH was measured using a pH meter Orion 410A, Cole Parmer, Vermon Hills, United States.

2.4.2. Kinematic viscosity

The viscosity was determined at 25 °C, using a capillary Cannon-Flenske Routine-type viscometer (Tube size 100, IVA), Cannon Instrument Company, State College, United States.

2.4.3. Drug–polymer relative composition

The drug content was determined by UV-spectrophotometry (UV-160A, Spectrophotometer, Shimadzu, Burladingen, Germany) at 319.5 nm. The UV absorption spectrum of PL:DX was employed to demonstrate that the polymers did not interfere with the IN quantification.

Considering that PL and DX are water soluble, the feed IN concentration (g_{IN}/mL) measured by UV was reported as $g_{IN}/g_{PL:DX}$ (Table 1) assuming that the PL:DX mass in the feed solutions was equal to the weighted polymer mixture used to prepare the $(PL–IN)_{50}$:DX Y% and $(PL–IN)_{25}$:DX 1.6% solutions. On the other hand, for the $(PL–IN)_{75}$:DX 1.6% fluid (where two phases were observed), the composition of the supernatant was reported (Table 1) using the concentration of IN and PL determined by UV and potentiometric titration (Section 2.2), respectively. The PL content in the supernatant was 97.17 ± 0.49% of the total PL:DX mass used for the $(PL–IN)_{75}$:DX 1.6% sample preparation.

All the above mentioned properties were measured by triplicate.

2.5. Spray drying

The aqueous solutions were atomized in a negative pressure lab-scale spray drier (Mini Spray Dryer B-290, BÜCHI, Flawil, Switzerland). A two-fluid nozzle with a cap-orifice diameter of 0.5 mm was used. Operating conditions were selected based on a previous work, air inlet temperature (co-current flow): 140 °C, drying air flow rate: 35 m^3/h, liquid feed flow rate: 6 mL/min and atomization air flow rate 601 L/h [20]. The process yield was calculated as the ratio of the weight of product obtained by SD respect to the feed solid content.

2.6. Particulate system characterization

2.6.1. Moisture content

After the SD process, moisture content of powders was determined in a halogen moisture analyzer (MB45, Ohaus, Pine Brook, United States). Around 500 mg of sample was heated up to 105 °C until the weight change was less than 1 mg in 60 s.

2.6.2. Drug load efficiency

The powders were dissolved in phosphate buffer pH 7.4 and drug concentration was measured by UV-spectrophotometry at 319.5 nm. The drug load efficiency was calculated as grams of drug per gram of powder. Since the sample moisture content is quantified, the IN load efficiency can also be expressed as $g_{IN}/g_{PL:DX}$.

2.6.3. Fourier transform infrared spectroscopy (FT-IR), powder X-Ray diffraction (PXRD) and differential scanning calorimetry (DSC)

2.6.3.1. FT-IR. SD powders and raw materials were studied in 1% w/w potassium bromide compacts, after being dried at 105 °C. A FT-IR instrument (Nexus FT, Thermo Nicolet, Maryland, United States) was used. The resulted spectrum was the average of 32 scans and 4% resolution.

2.6.3.2. PXRD. Sample diffractograms were recorded between the angles (2Θ) 5 and 60° (Rigaku, Geigerfleck, Tokyo, Japan), using an anodic cupper tube with a monochromator (35 kV and 15 mA). Angle and time steps of 0.04° and 0.8 s were selected, respectively.

Table 1
Theoretical and experimental composition, viscosity and pH of solutions for spray drying.

Sample	Theoretical formulation					Experimental solution properties			
	PL:DX (g)	IN (g)	IN concentration (% w/v)	Relative composition ($g_{IN}/g_{PL:DX}$)	Total solid content (% w/v)	Relative composition ($g_{IN}/g_{PL:DX}$)	Total solid content (% w/v)	Viscosity (mm^2/s)	pH
$(PL–IN)_{25}$:DX 1.6%	2.79	0.42	0.21	0.15	1.6	0.15 ± 0.01	1.6	1.65 ± 0.02	8.96 ± 0.08
$(PL–IN)_{50}$:DX 1.6%	2.47	0.74	0.37	0.30	1.6	0.28 ± 0.01	1.6	1.86 ± 0.02	8.54 ± 0.03
$(PL–IN)_{75}$:DX 1.6%[a]	2.20	1.01	0.51	0.46	1.6	0.34 ± 0.01	1.4	1.92 ± 0.03	8.36 ± 0.04
$(PL–IN)_{50}$:DX 0.6%	0.92	0.28	0.14	0.30	0.6	0.28 ± 0.01	0.6	–	8.14 ± 0.04
$(PL–IN)_{50}$:DX 1.3%	1.99	0.60	0.30	0.30	1.3	0.28 ± 0.01	1.3	1.49 ± 0.02	8.44 ± 0.03
$(PL–IN)_{50}$:DX 2.6%	4.00	1.20	0.60	0.30	2.6	0.28 ± 0.01	2.6	1.91 ± 0.03	8.76 ± 0.08
PL:DX 1.6%	3.21	–	–	–	1.6	–	1.6	1.69 ± 0.02	9.68 ± 0.08

Subscripts 25, 50 and 75 represent the theoretical PL neutralization degrees while the percentages indicate the theoretical total solid content.
[a] The experimental solution properties informed correspond to the supernatant with a total solid content of 1.4% w/v.

2.6.3.3. DSC. Weighted samples (~4 mg) were run at 10 °C/min ramp in closed aluminium pans under nitrogen atmosphere (40 mL/min) using a DSC equipment (Pyris 1, Perkin Elmer, Massachusetts, United States). A first heating from 30 to 180 °C, a cooling step from 180 °C to 30 °C and a second heating from 30 to 180 °C were performed. Glass transition temperature (*Tg*) for SD products and PL:DX as raw material was determined during the second heating by triplicate using the half ΔCp method [32]. The melting temperature (T_m and T_{onset}) and heat of fusion (ΔH_m) of pure IN and IN in the physical mixture PM were also determined.

2.6.4. Particle size distribution

The SD products were analyzed by laser diffraction (LA 950V2, Horiba, Kyoto, Japan, dry powder method) using a technique previously reported [20], where samples were dispersed in lactose (lactose:sample 6:1) to improve the powder flow from the feed hopper to the measuring cell. Complementarily, particle size distributions for raw IN, PL:DX and lactose were measured. Size is reported as median volumetric diameter (D_{50}) and the distribution width is informed as span (Eq. (1)).

$$Span = \frac{(D_{90} - D_{10})}{D_{50}} \quad (1)$$

where D_{10}, D_{50} and D_{90} are the diameters where the 10%, 50% and 90% of the population lies below each value, respectively. A distribution can be considered relatively narrow if the span value is less than 2 [20].

2.6.5. Particle morphology

A scanning electron microscope (SEM) (EVO 40-XVP, LEO scanning electron microscope, Oberchoken, Germany) was used to evaluate the material morphology. $(PL\text{-}IN)_x$:DX 1.6% and PL:DX 1.6% SD powders, and raw PL:DX and IN were assessed. Before analysis the samples were metalized with a thin layer of gold using a sputter coater (PELCO 91000, TellPella, Canada).

2.6.6. Particle and bulk density determination

The sample or skeletal density of the SD and raw powders was determined by nitrogen adsorption (Nova 1200e, Quantachrome Instruments, Florida, United States). 1 g sample was placed in a precalibrated cell and its volume was determined by nitrogen intrusion. The sample density was calculated as the solid mass divided by the volume of the particles excluding the open pores. For very porous particles and well-connected pores the sample density can be assumed to be close to the solid density, while for non-porous particles the sample density represents the particle one.

In order to determine bed densities of the spray-dried samples, the powder was gently poured into a 10 cm^3 graduated cylinder. Bulk density (D_{bulk}) was calculated as the ratio of the weight (g) of the sample contained in the cylinder to the volume occupied. Tap density (D_{tap}) was estimated by tapping the cylinder until no measurable change in volume was noticed. All determinations were made by triplicate. Carr Index (CI, Eq. (2)) was evaluated according to USP [33]:

$$CI = \left(D_{tap} - D_{bulk}\right) 100/D_{tap}. \quad (2)$$

Additionally the $(PL\text{–}IN)_{50}$:DX 1.6% sample was assayed with lactose as a carrier to improve flowability in a sample:carrier ratio of 1:3.

2.6.7. Estimated and experimental aerodynamic behavior

As a first approach, the particle aerodynamic diameters (D_{aer}) for all the formulations were calculated as follows [34]:

$$D_{aer} = D_{50}\sqrt{D_p} \quad (3)$$

where D_p is the particle density.

As mentioned previously, the sample density becomes equal to the particle density for non-porous particles. For porous powders, the sample density will be higher than the particle one. Therefore, the aerodynamic diameters calculated based on sample density are overestimated.

To assess the total amount of respirable particles of a given formulation, the particle volumetric distribution obtained by laser diffraction was affected by the square root of the skeletal density to obtain an approximate D_{aer} distribution. The respirable fraction is defined as the percentage of the population with D_{aer} lower than 5 μm [33].

Secondly, to assess in vitro the fraction of particles that effectively could reach the pulmonary membrane, the $(PL\text{–}IN)_{50}$:DX 1.6% sample was assayed in a Next Generation Impactor (NGI, Coplay, Nottingham, UK). To this purpose and to achieve and adequate dispersibility of the particles, the powder was mixed with lactose in a 1:3 ratio. A 3-size gelatine capsule was filled with 45 mg of the powder blend and it was placed in a Breezhaler® dry powder inhaler (Novartis). The NGI was operated at constant air flowrate (60 L/min) for 4 s. To prevent particle re-entrainment, the NGI stages were precoated with glycerine. The powder deposited on the NGI stages, inhaler, induction port and adapter was recovered with an appropriate volume of water and the amount determined by UV spectrophotometry at 319.5 nm. The respirable fraction (RF), mass median aerodynamic diameter (MMAD) and geometric standard deviation (GSD) were determined according to USP for apparatus 5 [33]. Experiments were done by duplicate.

2.7. Drug release experiments

The experiments were performed in vertical Franz Cells at 37 °C, where receptor and donor compartments were limited by a dialysis cellulose membrane (Sigma, molecular weight cut-off: 14,000 Da). The receptor compartment (60 mL) was completed with degasified medium: phosphate buffer pH 7.4 or water. Raw IN and $(PL\text{–}IN)_{50}$:DX 1.6% SD powder were dissolved in phosphate buffer pH 7.4. Additionally, the SD powder was dissolved in water. The donor compartment was filled with 5 mL of the prepared solutions. For all the solutions, the IN concentration was 2.5 mg/mL. Raw IN amount in donor compartment was limited by drug solubility in phosphate buffer pH 7.4 (2.75 mg/mL in buffer pH 7.4 at 37 °C [35]). The receptor compartment was maintained under magnetic stirring. 2 mL samples were withdrawn at constant intervals of 30 min up to 6 h and replaced with fresh medium. IN content in the samples was assayed by UV spectrophotometry at 319.5 nm. The experiments were performed by triplicate.

3. Results

3.1. Formation of complexes PL–IN in aqueous medium

When a cationic polyelectrolyte (R-NH_2) is combined with an acidic drug (D-COOH) in an aqueous medium, ionic pairs between them are generated according with Eqs. (4)–(6). The mechanism could be expressed as follows:

$$D{-}COOH \rightleftarrows D{-}COO^- + H^+ \quad (4)$$

$$R{-}NH_2 + H^+ \rightleftarrows R{-}NH_3^+ \quad (5)$$

$$D{-}COO^- + R{-}NH_3^+ \rightleftarrows \left[D{-}COO^-R{-}NH_3^+\right] \quad (6)$$

where *D-COOH* and *D-*COO^- represent a drug with carboxylic or carboxylate groups respectively; *R-*NH_2 and *R-*NH_3^+ represent the un-protonated and protonated polyelectrolyte species and [*D-*COO^-*R-*NH_3^+] represents the ionic pair or complex. Eq. (6) is known as counterion condensation in polyelectrolyte solutions [36]. This mechanism is postulated to represent the PL–IN interaction, which will be discussed in the following sections. With respect

to DX, it is assumed that this molecule does not interfere with the complex formation because the equilibrium properties are not modified by non-electrolytes [37].

3.2. $(PL–IN)_x$:DX solution characterization

As it can be seen in Table 1, the feed solutions were characterized before the spray drying process. pH, viscosity and IN content were evaluated for samples containing the $(PL–IN)_x$:DX complex with different neutralization degrees and solid contents. For the PL:DX 1.6% solution, pH and viscosity were also measured.

The PL:DX solution had a pH around 9.7, while for the complexes the pH varied from 8.14 to 8.96. The addition of the drug to the polymeric solution decreased the pH due to the PL amino group neutralization. For pH = 10, the reported IN solubility at room temperature and in water was less than 1 mg/mL [38]. For this reason, the IN solubility for pHs between 8.14 and 8.96 should be even lower than 1 mg/mL. For samples with a neutralization degree of 50%, the IN concentration varied from 1.3 to 5.6 mg/mL, experimental values well above the expected IN solubility. However, for all those samples the solutions obtained were translucent and pale yellow, without any evidence of saturation. The new entities $(PL–IN)_{50}$:DX Y% allow high IN loadings, beyond the pure IN solubility. For a constant solid content of 1.6%, also no solution saturation was observed for a neutralization degree of 25%. Conversely when the 75% of the PL amino groups were neutralized, the fluid was not homogeneous, distinguishing a darker yellow layer at the bottom. It is important to note that for $(PL–IN)_{75}$:DX 1.6% the IN concentration in the supernatant was 3.8 mg/mL, value lower than the one corresponding to the sample $(PL–IN)_{50}$:DX 2.6%. The $(PL–IN)_x$:DX complexes allow significantly higher IN loadings in aqueous solutions than the common strategy based on the medium alkalinization [39]. Besides, the proposed formulations increase the IN concentration without using organic solvents (like methanol) to dissolve this drug [40]. These results indicate that high IN concentrations in aqueous medium can be achieved if there are enough PL:DX material. Taking into account that these results are in agreement with the high increase in aqueous compatibility observed for other polyelectrolytes–non water soluble drugs [36,37] and that Limwikrant et al. [41] reported that IN is not solubilized by DX in the presence of water, the IN solubility enhancement is mainly associated with the PL–IN interaction.

Viscosity is known as a feed property that affects the SD process. When the feed solution viscosity increases, the atomized droplets become larger and therefore the dry performance decreases [42]. In order to evaluate if solutions were adequate to be atomized, kinematic viscosity was measured. According to the viscosities listed in Table 1, the values are at the most 30% higher than the water kinematic viscosity at 25 °C. Then, the atomization of the feed solutions would not introduce operating problems. For the solutions containing the complexes and for a given neutralization degree, in agreement with Frascareli et al. [42], the higher the solid content the higher the viscosity values.

For all the solutions containing complexes and neutralization degrees of 25 and 50%, the IN relative composition (experimental value) was in good agreement with the expected concentration (theoretical value). However, for $(PL–IN)_{75}$:DX 1.6% the experimental concentration of an aliquot withdrawn from the supernatant liquid was about 74% of the expected value (0.46 $g_{IN}/g_{PL:DX}$). For this sample, the fact that it was not possible to obtain a homogeneous solution explains the difference observed between the theoretical and experimental IN relative compositions.

3.3. Spray drying process

In Table 2 the SD outlet air temperature and yield are listed for all the performed experiments, it also shows some properties (moisture content, relative composition and load efficiency) of the obtained powders.

The outlet air temperature (T_{out}) of the spray drying process is known to affect the stability of labile compounds. In this work, T_{out} was between 70.5 and 86.0 °C. As IN is thermally stable up to 248 °C, this compound is processed well below its degradation temperature [43]. Regarding PL, 5% w/v aqueous solutions of this polymer were previously spray dried by Maurer and Lee at an inlet temperature of 150 °C without degradation signals [44]. Since in this work the air inlet temperature was 140 °C and the solid content was lower than 5%, no thermal degradation for PL is expected.

The process yields were between 42 and 67 wt.%, being acceptable values for lab-scale driers. The yield decreased as the neutralization degree increased. This result could be related to stickiness of the samples to the chamber wall. Stickiness is usually related to the material glass transition temperature (*Tg*) [20]. As it can be seen in Table 3, the *Tg* for samples $(PL–IN)_x$:DX 1.6% decreased as neutralization degree increased, this result is in good agreement with the process yields found for those samples. Particularly, for the $(PL–IN)_{75}$:DX 1.6% the yield decrease could be also associated with the actual solid content in the liquid solution fed to the spray drier (1.4%). However as it is shown below, low changes of solid content did not affect the process yield.

For a constant neutralization degree, the process yield did not change significantly when the total solid content was varied from 1.3 to 1.6% due to the low variation in this operating condition. Just to test the effect of the total solid content on the process yield, this parameter was drop to 0.6%, for this case the yield decreased to 42%. However, when the total solid content increased from 1.6 to 2.6%, the process yield was improved by 34%. Then, as expected as the solid content is increased, the drying performance is improved [45,20].

3.4. Product characterization

3.4.1. Moisture content and drug load efficiency

The moisture content of the powders obtained by SD is also shown in Table 2. Values ranged from 3.50 to 5.00%, adequate results for a lab-scale SD unit. The particles obtained from the sample $(PL–IN)_{50}$:DX 2.6% presented, besides the highest yield, the lowest moisture content. This behavior can be attributed to the lowest water content in the atomized droplets [46].

The drug load efficiency was determined by quantifying the IN content by UV in the SD powders (see Table 2). From these data, and considering that the powders are constituted by IN, PL:DX and moisture,

Table 2
SD outlet air temperature and yield and moisture, relative composition and load efficiency of products.

Sample	T_{out} (°C)	Yield (%)	Moisture (%)	Relative composition ($g_{IN}/g_{PL:DX}$)	Load efficiency (g_{IN}/g_{solid})
$(PL–IN)_{25}$:DX 1.6%	69.0 ± 0.0	54.38 ± 2.35	4.68 ± 0.25	0.14	0.12 ± 0.01
$(PL–IN)_{50}$:DX 1.6%	74.0 ± 4.5	50.10 ± 1.63	4.83 ± 0.36	0.27	0.20 ± 0.01
$(PL–IN)_{75}$:DX 1.6%	70.5 ± 0.7	46.23 ± 3.83	4.84 ± 0.34	0.35	0.26 ± 0.01
$(PL–IN)_{50}$:DX 0.6%	–	42.20[a]	–	–	–
$(PL–IN)_{50}$:DX 1.3%	85.0[a]	51.25[a]	4.57[a]	0.27	0.20 ± 0.01
$(PL–IN)_{50}$:DX 2.6%	80.0[a]	67.18[a]	3.50[a]	0.25	0.19 ± 0.01
PL:DX 1.6%	72.0 ± 0.0	46.86 ± 1.35	5.00 ± 0.12	–	–

T_{out}: outlet air temperature.
[a] Single determinations.

Table 3
Thermal behavior of raw materials, SD powders and PM.

Sample	*Tg* (°C)	T_m (°C)	T_{onset} (°C)	ΔH_m (J/g_{IN})
$(PL–IN)_{25}$:DX 1.6%	138.50 ± 1.09	–	–	–
$(PL–IN)_{50}$:DX 1.6%	128.31 ± 1.79	–	–	–
$(PL–IN)_{75}$:DX 1.6%	126.07 ± 3.22	–	–	–
$(PL–IN)_{50}$:DX 2.6%	127.12 ± 2.23	–	–	–
PL:DX	145.24 ± 1.75	–	–	–
PL:DX 1.6%	139.64 ± 2.87	–	–	–
PM	–	161.28	158.96	65.45
IN	53.22 ± 2.00	163.24	159.99	108.94

T_m, T_{onset} and ΔH_m were determined during the first heating.

the relative composition of IN expressed as $g_{IN}/g_{PL:DX}$ was calculated for all the samples. Except for the sample $(PL–IN)_{50}$:DX 2.6%, the powder relative IN composition is in very good agreement with drug content found in the feed solutions (Table 1). The $(PL–IN)_{50}$:DX 2.6% powder presented a relative IN content 11% lower than the expected value, nevertheless this difference is consider as acceptable [47].

3.4.2. FT-IR characterization

For powder characterization at molecular level, FT-IR spectra of the SD materials were obtained. The analyzed samples were: $(PL–IN)_x$:DX 1.6% and PL:DX 1.6% SD powders and the pure raw materials. The FT-IR study was addressed to study the ionic interaction between PL amino groups and IN carboxylic groups. Fig. 2 shows the FT-IR spectra for representative samples, relevant bands were highlighted at around the following wavenumbers:

- 900 and 1720 cm^{-1} corresponding to the non-dissociated acidic groups [48,23], and
- 1590 cm^{-1} representative of the dissociated amino groups [49].

The spectra of the raw PL:DX and the spray-dried PL:DX 1.6% powder showed similar FT-IR profile, indicating that the spray-drying process did not degrade the PL-DX sample. Consequently, only the spectrum of the PL:DX 1.6% powder was included in Fig. 2. According to Maurer and Lee, [44] the main PL characteristic signal ("amide I band") appears at 1642 cm^{-1}. In a good agreement, the PL:DX 1.6% sample exhibited a relatively wide band at around 1656 cm^{-1} (non-highlighted signal, see Fig. 2). For the PL:DX system the signal associated with the $-NH_2$ group could not be identified because it is overlapped by the PL amide signal and DX OH signal.

As expected, the stretching of COOH group and out of plane stretching of O – H group of carboxylic acid were detected in the pure IN spectrum at 1721 and 905 cm^{-1}, respectively (Fig. 2). As IN is always the limiting reactant and as a proof of an almost complete reaction, these two signals completely disappeared for all the $(PL–IN)_x$:DX 1.6% samples; simultaneously a tiny band became visible at 1589.7, 1591.9 and 1590.1 cm^{-1} for $(PL–IN)_x$:DX 1.6% for x varying from 25 to 75%, respectively. This signal is ascribed to the asymmetric wagging of NH_3^+. The bands associated with COO^- symmetric (~1400 cm^{-1}) and asymmetric (1630–1660 cm^{-1}) stretching and NH_3^+ symmetric wagging (1470–1480 cm^{-1}) could not be unequivocally identified because them and the signals ascribed to IN indole group stretching (1481 cm^{-1}) [48] and deformation (1408 cm^{-1}) and stretching (1635 cm^{-1}) of the DX OH groups are overlapped [50]. Besides, the presence of the signal ascribed to asymmetric wagging of NH_3^+, suggests the PL–IN interaction.

3.4.3. Crystallographic characterization

To evaluate the IN crystalline changes due to the SD process and feed composition, the same samples studied by FT-IR were assessed by PXRD. Also, a physical mixture (PM) of PL:DX and IN at the same ratio than the one employed for the preparation of sample $(PL–IN)_{50}$:DX 1.6% was studied. Since the material crystallinity can change over storage time, an aged $(PL–IN)_{50}$:DX 1.6% sample (9 months, room temperature) was also assessed by PXRD. All the diffractograms are displayed in Fig. 3.

Accordingly with the IN diffractogram pattern (Fig. 3a), the pure drug displayed crystalline structure; the position and intensity of reflections were in good agreement with reported data [10]. 100-relative intensity peak was found at 19.76° (interplanar distance of 4.49 Å), being the pattern consistent with the IN polymorph ϒ or I, which is the most stable state [10]. Regarding the raw and SD PL:DX samples, the diffractograms confirm that both materials were amorphous (Fig. 3a); indeed no peaks and base-line elevation were detected [20].

The PM pattern (Fig. 3b) showed both the characteristic peaks associated with the IN crystalline structure and the baseline elevation that is representative of the PL:DX amorphous state. However, the sample $(PL–IN)_{50}$:DX 1.6% exhibited an amorphous pattern. This amorphicity can be attributed to either the SD process or the ionic interaction between PL and IN, or both. Ceschan et al. demonstrated for the alginic acid–atenolol system that the interaction between the drug and the polyelectrolyte caused the drug crystallinity lost in powder obtained by SD [20]. For a constant solid content, the neutralization degree did not qualitatively modify the PXR diffractograms (Fig. 3b), therefore the material structure is not influenced by the tested feed compositions.

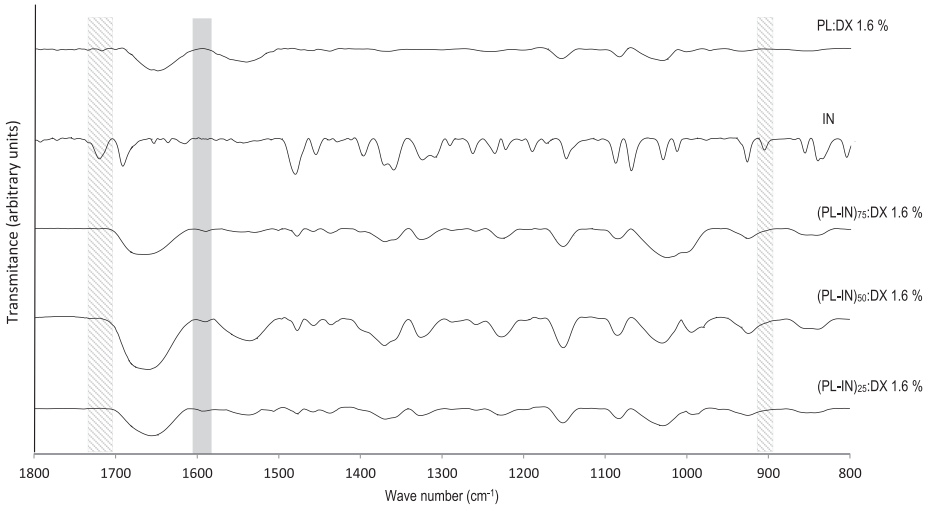

Fig. 2. FT-IR spectra of $(PL–IN)_x$:DX 1.6%, PL:DX 1.6% and raw IN. Relevant bands are highlighted (dashed fill bar: non-dissociated acidic groups of IN; solid bar: dissociated amino groups).

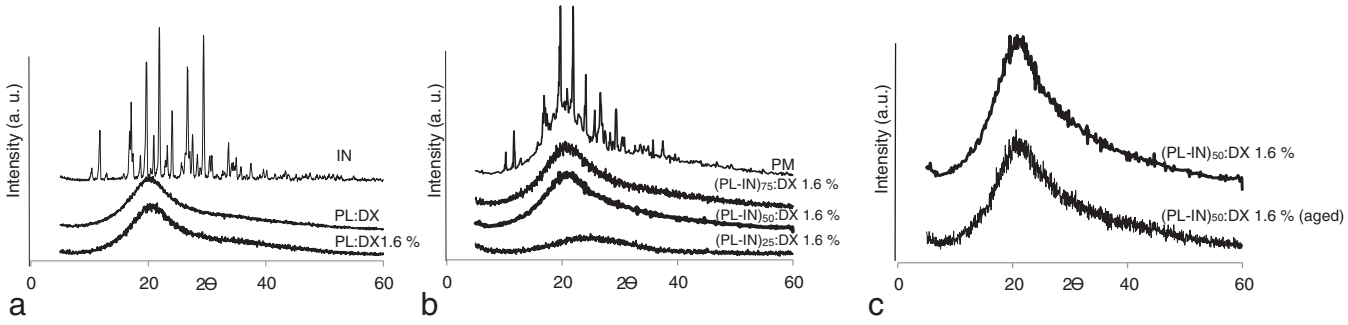

Fig. 3. PXRD patterns: a) Raw and SD PL:DX and raw IN, b) PM and $(PL–IN)_x$:DX 1.6%, c) Fresh and nine months stored $(PL–IN)_{50}$:DX 1.6% samples. a.u.: arbitrary units.

For poor water soluble drugs, such as IN, the amorphous state is preferred to improve their bioavailability [31,48]. Therefore, the new particulate formulations proposed in this work, based on the interaction between the drug and a polyelectrolyte and the use of a simple processing technique, allows the production of totally amorphous materials.

Several authors investigated the production of amorphous IN ystems, however the amorphous material tended to crystallize over time [51]. Among others, Ewing et al. developed a solid dispersion of IN–polyethylene glycol by a hot-melt method followed by quench cooling. Initially, IN in the samples was completely amorphous, but after four days, the IN crystallized to the ϒ-solid structure [52]. With the purpose of studying the stability of the complexes obtained by SD and based on polyelectrolyte–drug interaction, the sample $(PL–IN)_{50}$:DX 1.6% was stored during nine months. As can be seen in Fig. 3c, the aged $(PL–IN)_{50}$:DX 1.6% sample remained as amorphous material after storage period. The pure IN crystallization is dominated by the formation of hydrogen bonds between carboxylic groups of two IN molecules. Then, nucleation starts when IN dimers are formed [53]. According to the FT-IR results, the absence of IN non-dissociated carboxylic groups for the $(PL–IN)_{50}$:DX 1.6% sample indicates that the dimer formation could not be feasible, consequently the crystallization would be limited by the PL–IN interaction.

3.4.4. Thermal analysis

The materials studied by PXRD were also thermally analyzed by DSC. Fig. 4a shows the pure IN thermogram while Fig. 4b displays the thermograms corresponding to the complexes $(PL–IN)_x$:DX 1.6%, PM and the SD PL:DX. Table 3 reports the glass transition temperature, melting temperatures and heats for different samples thermally treated.

An endothermic event at 163.24 °C was detected in the IN first heating. The temperatures 155 °C and 161 °C were reported as the melting points for the IN polymorphic forms α and γ, respectively [10]. According to this, the IN raw material state corresponded to the polymorphic form γ. This result agrees with the diffractogram pattern already discussed in the previous section. For IN, the melting peak did not appear during the second heating (Fig. 4a). This behavior was related to the absence of IN crystallization during cooling step and in agreement with the observation reported by Shimada et al. [54]. The measured IN *Tg* was 53.22 °C. Since the storage at temperatures near IN *Tg* allows molecular mobility of the drug and hence nucleation and crystallization [52], partial IN recrystallization could be expected at room conditions [52].

During the first heating, the SD PL:DX showed an endothermic event nearly 100 °C (which can be associated with the adsorbed water loss) and the absence of melting peaks, result that is in good agreement with the observed amorphous PXRD pattern (Fig. 3a).

The PM sample showed two endothermic events during the first heating (Fig. 4b). One wide endotherm at approximately 100 °C, attributed to the adsorbed water elimination, and the drug melting peak at 161.3 °C (see Table 3). IN melting temperature in the PM was slightly lower than the one found for pure IN (Table 3), this is an expected result for non-pure materials [55]. Moreover, the melting heat (expressed by IN grams) for PM was about 60% of the corresponding value for pure IN, indicating that a partial interaction between the components of PM takes place [55].

For the powders $(PL–IN)_x$:DX 1.6%, only an endothermic event around 100 °C was observed, consistent with the loss of adsorbed water. Besides, for all these samples, the IN melting peak did not appear. This is in good agreement with the absence of crystalline structure observed in $(PL–IN)_x$:DX 1.6% diffractograms (Fig. 3b). Moreover, the glass transition temperatures for all the $(PL–IN)_x$:DX 1.6% powders were above 100 °C (Table 3), values markedly higher than the pure IN *Tg*. As mentioned previously, low *Tg* allows (at room conditions)

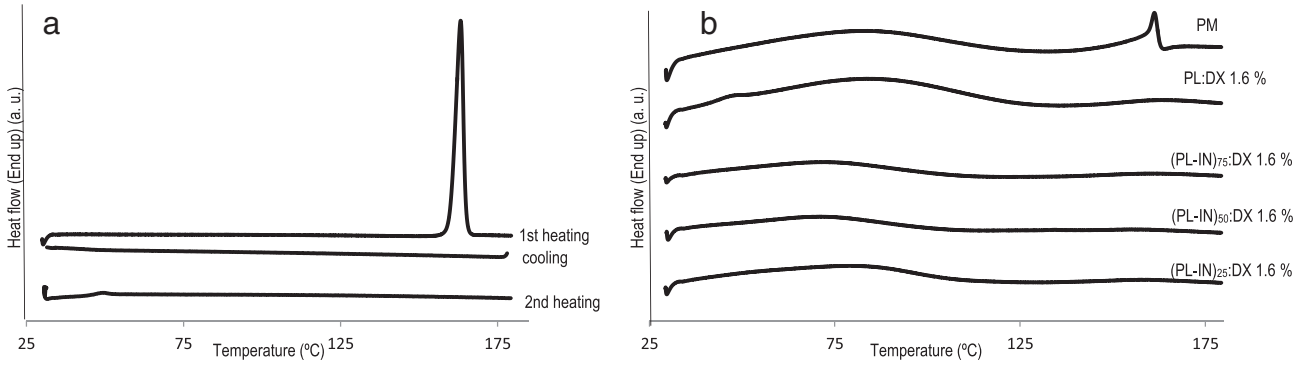

Fig. 4. DSC thermograms of a) pure IN and b) PM, PL:DX 1.6% and $(PL–IN)_x$:DX 1.6% powders. a. u.: arbitrary unit.

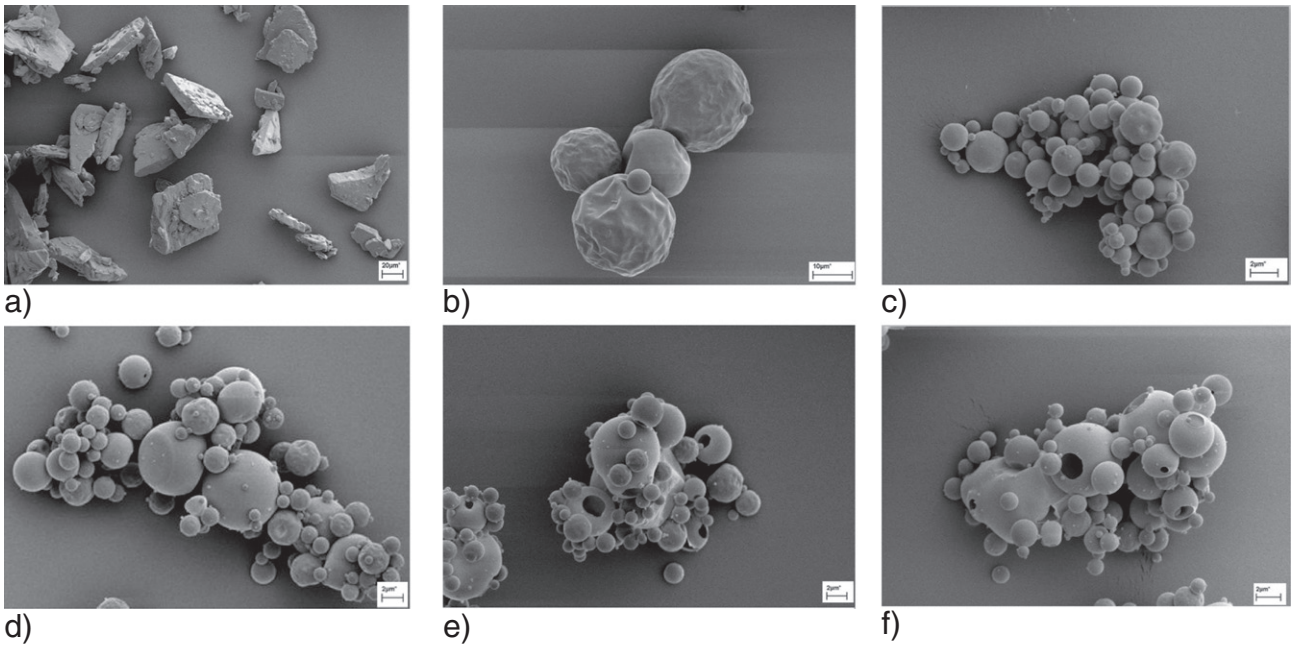

Fig. 5. SEM micrographs. a) pure IN (800×), b) raw PL:DX (3000×), c) PL:DX 1.6% (10,000×), d) $(PL–IN)_{25}$:DX 1.6% (8000×), e) $(PL–IN)_{50}$:DX 1.6% (8000×) and f) $(PL–IN)_{75}$:DX 1.6% (10,000×).

molecular mobility and nucleation. The proposed system admits high amounts of IN keeping the amorphous state with a relatively high *Tg*, facilitating manipulation and storage at room conditions.

3.4.5. Morphology and particle size distribution

To study the effect of the SD feed formulation on the particle morphology, the powders were analyzed by scanning electronic microscopy (SEM). Fig. 5 shows the micrographs corresponding to the raw materials and the SD powders obtained by spraying the $(PL–IN)_x$:DX 1.6% and PL:DX 1.6% solutions. Also, the granulometry of the powders was determined by laser diffraction, Table 4 reports median of the volumetric size distribution as well as the distribution width expressed as span.

Fig. 5a indicates that the morphology of IN particles was consistent with plate crystals, particle appearance that is in good agreement with the morphology reported by Bandi et al. [56].

The raw PL:DX showed particles (Fig. 5b) with rounded shape and dented surface. As can be seen in Fig. 5c, the SD PL:DX 1.6% powder was constituted by agglomerated, rounded and smooth surface particles. Besides, the particle size of the SD PL:DX system were significantly smaller and the particle size distribution was narrower than its raw material (see Table 4).

For the $(PL–IN)_x$:DX 1.6% powders, mainly rounded smooth particles were obtained. No crystals were observed in concordance with the amorphous pattern confirmed by PXRD. The SD particles exhibited some holes indicating a probable hollow structure, which is very attractive for inhalatory applications.

Table 4
Median diameter, span, Carr index (*CI*) and solid density of SD products and pure materials.

Sample	D_{50} (μm)	Span	*CI*	Density (g/cm^3)
$(PL–IN)_{25}$:DX 1.6%	6.59 ± 0.23	1.13	37.81 ± 0.48	0.73 ± 0.06
$(PL–IN)_{50}$:DX 1.6%	5.99 ± 0.27	1.05	37.38 ± 0.55	0.64 ± 0.03
$(PL–IN)_{75}$:DX 1.6%	6.97 ± 0.45	1.02	37.67 ± 0.93	0.62 ± 0.05
$(PL–IN)_{50}$:DX 1.3%	6.04 ± 0.37	1.04	36.64 ± 0.51	0.69 ± 0.06
$(PL–IN)_{50}$:DX 2.6%	5.95 ± 0.18	1.06	37.84 ± 0.46	0.68 ± 0.05
PL:DX	68.29 ± 2.97	1.96	–	0.99 ± 0.02
PL:DX 1.6%	4.78 ± 0.39	1.04	–	0.77 ± 0.10
IN	58.57 ± 7.94	3.26	–	1.11 ± 0.05

Regarding to particle size distribution, $(PL–IN)_x$:DX systems presented volumetric median diameters between 5.95 and 6.97 μm (Table 4). No significant differences were found related to the neutralization degree or solid content in feed solution. Besides, narrow distributions were obtained as indicated by low span values, also shown in Table 4.

3.4.6. Flow properties

Table 4 also shows the Carr Index for the different $(PL–IN)_x$:DX Y% SD samples. According to the USP powder classification, the powders presented very poor flow properties [33]. This result agrees with the behavior of small particles. It has been described that van der Waal forces dominate the particle–particle interaction and that flow can be improved using carrier particles, like lactose. For this reason, $(PL–IN)_{50}$:DX 1.6% was mixed with lactose in a ratio $(PL–IN)_{50}$:DX 1.6%:lactose 1:3. Carr Index was measured and the determined value was 26.95%. This flow is classified as acceptable. Thus, the powder flowability can be improved using a carrier like lactose [57].

3.4.7. Powder density

As also shown in Table 4, the SD powder skeletal densities were between 0.62 and 0.73 g/cm^3, values that are well below that those found for IN and PL:DX raw materials, which presented densities of 1.11 and 0.99 g/cm^3, respectively. Considering that SD systems were less dense than their precursor materials, the particles should have a hollow structure as suggested by the SEM micrographs.

Table 5
Calculated median aerodynamic diameter (D_{aer}) and cumulative respirable fraction.

Sample	Median D_{aer} (μm)	Volume cumulative fraction with D_{aer} lower than 5 μm (%)
$(PL–IN)_{25}$:DX 1.6%	5.63	38.97 ± 0.38
$(PL–IN)_{50}$:DX 1.6%	4.79	51.55 ± 0.37
$(PL–IN)_{75}$:DX 1.6%	5.49	44.43 ± 0.43
$(PL–IN)_{50}$:DX 1.3%	5.02	41.56 ± 0.46
$(PL–IN)_{50}$:DX 2.6%	4.91	49.39 ± 0.49

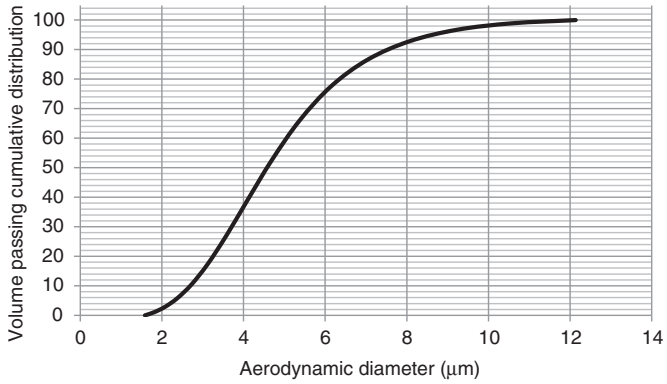

Fig. 6. Volume passing cumulative distribution for $(PL–IN)_{50}$:DX 1.6%.

3.4.8. Aerodynamic behavior

In this work, estimated D_{aer} was calculated accordingly Eq. (3) and are shown in Table 5. The median D_{aer} values were between 4.79 and 5.63 μm. However the knowledge of the whole D_{aer} distribution is necessary to evaluate the powder quality for inhalatory applications. In fact, Table 5 indicates that the respirable fraction for all samples was above 39%. According to this result, the $(PL–IN)_{50}$:DX 1.6% sample appears to have better attributes to be administrated by inhalation. Fig. 6 shows the volume passing cumulative distribution as a function of the estimated aerodynamic diameters for this sample. As it can be seen, the population is distributed between aerodynamic diameters of 1.58–12.13 μm and 51.55% of it is located within the respirable region.

In order to demonstrate in vitro the fraction of particles with the capability to reach the pulmonary membrane, the $(PL–IN)_{50}$:DX 1.6% sample was also assessed using a NGI equipment. The RF, i.e. particles with an aerodynamic diameter lower than 5 μm with respect to the mass entering the NGI, was 73.50 ± 2.23%. This parameter represents the mass of drug that effectively could reach the respiratory membrane. The MMAD, i.e. the aerodynamic diameter where the 50% of the particle population lies below, was 3.36 ± 0.17 μm and the GSD 2.05 ± 0.02 μm. This result confirmed that the tested material is adequate to target IN to the respiratory membrane [58]. On the other hand, as expected, the estimated median D_{aer} (by Eq. (3)) and the respirable fraction based on this diameter are overestimated and underestimated, respectively. However, it is an interesting method to perform sample screening during the development stage of products.

3.5. In vitro IN release

Between all the powders obtained by SD, the $(PL–IN)_{50}$:DX Y % formulations became as the more attractive particulate systems, because they had a relative high load efficiencies without presenting saturation problems in the feed preparation step. As all the $(PL–IN)_{50}$:DX Y% samples had almost the same load efficiency (see Table 2), it is expected that the dissolution of a given amount leads to very similar IN concentrations in aqueous media. Therefore, in vitro drug release experiments were performed using the formulation $(PL–IN)_{50}$:DX 1.6%.

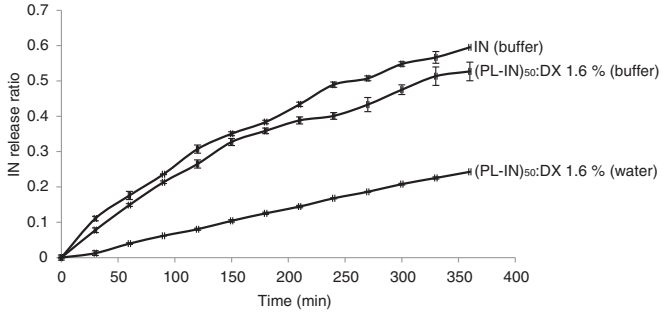

Fig. 7. Drug release from $(PL–IN)_{50}$:DX 1.6% and IN aqueous solutions towards distilled water and buffer pH 7.4.

Fig. 7 shows the drug release profiles for the $(PL–IN)_{50}$:DX 1.6% sample in phosphate buffer pH 7.4 and in pure water, as well as the pure IN profile in phosphate buffer. Particularly, the aim of the drug release study was to evaluate the dissociation capability of the complex dissolved in different relevant media. The phosphate buffer was selected to simulate pulmonary physiological conditions; while water was used for comparative purposes (it approximates the SD feed environment).

The developed complexes can undergo different reactions according to the nature of the release medium. Eq. (7) shows the reversible dissociation that takes place when the complex is dissolved in pure water.

$$R{-}NH_3{}^{+}D{-}COO^{-} \overset{H_2O}{\rightleftarrows} R{-}NH_2 + D{-}COOH \cdot \tag{7}$$

Using an aqueous medium, the IN transport from the donor compartment to the receptor one was relatively slow. In fact, after 6 h only the 24% of the initial IN contained in the complex was transferred through the cellulose membrane. The low initial release suggested a low dissociation equilibrium constant, or in other words, the presence of a high proportion of ionic pairs with respect to the dissociated species in the donor medium [23].

When a buffer potassium phosphate medium is employed, the system can undergo the following reaction:

$$R{-}NH_3^{+}D{-}COO^{-} + H_2PO_4^{-} + K^{+} \rightleftarrows R{-}NH_3^{+}H_2PO_4^{-} + D{-}COO^{-}K^{+}. \tag{8}$$

where PO_4^{-} and K^{+} represent the ions present in the solution [23].

As it can be seen in Fig. 7, when the experiment was performed using the phosphate buffer at pH 7.4, a faster initial IN transport with respect to the one observed for pure water was detected. This result suggested that the equilibrium favors the complex dissociation. After 6 h, almost the 53% of the initial IN present in the dissolved complex was transported through the membrane. This value is close to the release percentage exhibited by the pure drug (59%), then the complex dissociation was confirmed. Afterward, the reversibility of the PL–IN interaction is feasible.

4. Conclusions

In this work, a novel product for inhalatory targeting of indomethacin was developed by a simple processing technique (spray drying). Based on aqueous feed solutions (containing the drug and polylysine), the use of organic solvents was avoided. Due to the PL–IN interaction and the existence of free PL amino groups, the developed PL–IN formulations allowed relatively high IN loadings in aqueous solutions. For all the tested formulations $(PL–IN)_x$:DX Y%, the FT-IR analysis, due to the presence of the signal ascribed to asymmetric wagging of NH_3^{+} and the disappearance of the bands related to the IN acidic groups, suggested the PL–IN interaction. The developed materials were amorphous and, particularly, $(PL–IN)_{50}$:DX 1.6% demonstrated to retain its amorphicity over nine months of storage. Moreover, the ionic interaction between polylysine and IN can be shifted to the non-dissociated drug form in physiological media, indicating that the interaction is reversible.

Among all the tested formulations, the particle systems $(PL–IN)_{50}$:DX Y% were the more attractive ones, because they had a relative high load efficiencies without presenting saturation problems in the feed preparation step. For a neutralization degree of 50% and a constant desired production, the lower the solid content the higher the processing times and energy costs. In this sense, the powders $(PL–IN)_{50}$:DX 1.6%

(which exhibited the highest respirable fraction) and 2.6% (that presented the highest process yield) are good candidates. Further studies, such as dissolution, microparticles–carrier interaction and pulmonary bioavailability evaluation, are necessary to optimize the formulations for inhalatory treatment of the rheumatoid arthritis.

Finally and taking into account the improved properties of the studied materials, the information provided by this work could be useful as a starting point for the development of spray-dried powders based on cationic polyelectrolyte and poor soluble drug complexes, as particulate platforms of drug delivery for inhalable or other administration routes.

Acknowledgments

FONCyT (PICT-PRH 2009-0124), CONICET (PIP 112-2011-0100336 112) and UNS (PGI 24/B209) grants support this study. N.E.C. thanks CONICET for her doctoral fellowship. The authors thank Purac America for kindly supplying the PL:DX sample and Lic. F. Cabrera (PLAPIQUI) for her technical assistance.

References

[1] M. Feria, Fármacos analgésicos-antitérmicos y antiinflamatorios no esteroideos. Antiartríticos, in: Jesús Florez, Juan Antonio Armijo, África Mediavilla (Eds.), Farmacología Humana, 1997, pp. 355–387.
[2] T. Picot, B. Hamid, Decision-making in the cancer pain setting: beyond the WHO ladder, Tech. Reg. Anesth. Pain Manag. 14 (2010) 19–24. http://dx.doi.org/10.1053/j.trap.2009.12.003.
[3] A. Lanas, Efectos secundarios gastrointestinales por antiinflamatorios no esteroideos y costes en el Sistema Nacional de Salud, An. Med. Interna 18 (2001) 561–563.
[4] A. Alhalaweh, S. Andersson, S.P. Velaga, Preparation of zolmitriptan–chitosan microparticles by spray drying for nasal delivery, Eur. J. Pharm. Sci. 38 (2009) 206–214. http://dx.doi.org/10.1016/j.ejps.2009.07.003.
[5] M. Stigliani, R.P. Aquino, P. Del Gaudio, T. Mencherini, F. Sansone, P. Russo, Non-steroidal anti-inflammatory drug for pulmonary administration: design and investigation of ketoprofen lysinate fine dry powders, Int. J. Pharm. 448 (2013) 198–204. http://dx.doi.org/10.1016/j.ijpharm.2013.03.030.
[6] A. Pomázi, R. Ambrus, P. Sipos, P. Szabó-Révész, Analysis of co-spray-dried meloxicam — mannitol systems containing crystalline microcomposites, J. Pharm. Biomed. Anal. 56 (2011) 183–190. http://dx.doi.org/10.1016/j.jpba.2011.05.008.
[7] A.A. Onischuk, T.G. Tolstikova, I.V. Sorokina, N.A. Zhukova, A.M. Baklanov, V.V. Karasev, et al., Analgesic effect from Ibuprofen nanoparticles inhaled by male mice, J. Aerosol Med. Pulm. Drug Deliv. 22 (2009) 245–253. http://dx.doi.org/10.1089/jamp.2008.0721.
[8] M. El-Badry, G. Fetih, M. Fathy, Improvement of solubility and dissolution rate of indomethacin by solid dispersions in Gelucire 50/13 and PEG4000, Saudi Pharm. J. 17 (2009) 217–225. http://dx.doi.org/10.1016/j.jsps.2009.08.006.
[9] P.J. Salústio, G. Feio, J.L. Figueirinhas, J.F. Pinto, H.M. Cabral Marques, The influence of the preparation methods on the inclusion of model drugs in a beta-cyclodextrin cavity, Eur. J. Pharm. Biopharm. 71 (2009) 377–386.
[10] R.T.Y. Lim, W.K. Ng, R.B.H. Tan, Dissolution enhancement of indomethacin via amorphization using co-milling and supercritical co-precipitation processing, Powder Technol. 240 (2013) 79–87. http://dx.doi.org/10.1016/j.powtec.2012.07.004.
[11] P.J. Stewart, F.-Y. Zhao, Understanding agglomeration of indomethacin during the dissolution of micronised indomethacin mixtures through dissolution and de-agglomeration modeling approaches, Eur. J. Pharm. Biopharm. 59 (2005) 315–323.
[12] J.Y. Kim, Y.S. Ku, Enhanced absorption of indomethacin after oral or rectal administration of a self-emulsifying system containing indomethacin to rats, Int. J. Pharm. 194 (2000) 81–89.
[13] Y.W. Chien, H. Xu, C.-C. Chiang, Y.-C. Huang, Transdermal controlled administration of indomethacin. I. Enhancement of skin permeability, Pharm. Res. 5 (1988) 103–106.
[14] Z.-L. Huang, M. Kagoshima, E. Kagawa, H. Shimada, Absoption of indometacin from nasal cavity in rats, Acta Pharmacol. Sin. 16 (1995) 117–120.
[15] H.Y. Karasulu, Z.E. Sanal, S. Sözer, T. Güneri, G. Ertan, Permeation studies of indomethacin from different emulsions for nasal delivery and their possible anti-inflammatory effects, AAPS PharmSciTech 9 (2008) 342–348. http://dx.doi.org/10.1208/s12249-008-9053-9.
[16] A. Amital, D. Shitrit, Y. Adir, The lung in rheumatoid arthritis, Presse Med. 40 (2011) e31–e48. http://dx.doi.org/10.1016/j.lpm.2010.11.003 (Paris, France: 1983).
[17] A. a Onischuk, T.G. Tolstikova, I.V. Sorokina, N. a Zhukova, A.M. Baklanov, V.V. Karasev, et al., Anti-inflammatory effect from indomethacin nanoparticles inhaled by male mice, J. Aerosol Med. Pulm. Drug Deliv. 21 (2008) 231–243. http://dx.doi.org/10.1089/jamp.2007.0672.
[18] F. Buttini, P. Colombo, A. Rossi, F. Sonvico, G. Colombo, Particles and powders: tools of innovation for non-invasive drug administration, J. Control. Release 161 (2012) 693–702. http://dx.doi.org/10.1016/j.jconrel.2012.02.028.
[19] A. Chow, H. Tong, P. Chattopadhyay, B. Shekunov, Particle engineering for pulmonary drug delivery, Pharm. Res. 24 (2007) 411–437. http://dx.doi.org/10.1007/s11095-006-9174-3.
[20] N.E. Ceschan, V. Bucalá, M.V. Ramírez-Rigo, New alginic acid-atenolol microparticles for inhalatory drug targeting, Mater. Sci. Eng. C 41 (2014) 255–266. http://dx.doi.org/10.1016/j.msec.2014.04.040.
[21] S. Shukla, A. Singh, A. Kumar, A. Mishra, Review on production and medical applications of -polylysine, Biochem. Eng. J. 65 (2012) 70–81. http://dx.doi.org/10.1016/j.bej.2012.04.001.
[22] Z. Kadlecova, Y. Rajendra, M. Matasci, L. Baldi, D.L. Hacker, F.M. Wurm, et al., DNA delivery with hyperbranched polylysine: a comparative study with linear and dendritic polylysine, J. Control. Release 169 (2013) 276–288. http://dx.doi.org/10.1016/j.jconrel.2013.01.019.
[23] D. Quinteros, V. Ramirez Rigo, A. Jimenez Kairuz, M.E. Olivera, R.H. Manzo, D. Allemandi, Interaction between a cationic polymethacrylate (Eudragit E100) and anionic drugs, Eur. J. Pharm. Sci. 33 (2008) 72–79. http://dx.doi.org/10.1016/j.ejps.2007.10.002.
[24] S.M. Hwang, D. Kim, S.J. Chung, C.K. Shim, Delivery of ofloxacin to the lung and alveolar macrophages via hyaluronan microspheres for the treatment of tuberculosis, J. Control. Release 129 (2008) 100–106.
[25] K. Kho, W.-S. Cheow, R.-H. Lie, K. Hadinoto, Aqueous re-dispersibility of spray-dried antibiotic-loaded polycaprolactone nanoparticle aggregates for inhaled anti-biofilm therapy, Powder Technol. 203 (2010) 432–439.
[26] K. Kho, K. Hadinoto, Dry powder inhaler delivery of amorphous drug nanoparticles: effects of the lactose carrier particle shape and size, Powder Technol. 233 (2013) 303–311. http://dx.doi.org/10.1016/j.powtec.2012.09.023.
[27] E.J. Lee, S.W. Lee, H.G. Choi, C.K. Kim, Bioavailability of cyclosporin A dispersed in sodium lauryl sulfate-dextrin based solid microspheres, Int. J. Pharm. 218 (2001) 125–131 (http://www.ncbi.nlm.nih.gov/pubmed/11337156).
[28] L. Huybrechts, WO2006117029A1. Use of polylysine in combination with either green tea or olive extracts or both for use against halitosis, 2006.
[29] M. Alsaadi, J.L. Italia, A.B. Mullen, M.N.V.R. Kumar, A.A. Candlish, R.A.M. Williams, et al., The efficacy of aerosol treatment with non-ionic surfactant vesicles containing amphotericin B in rodent models of leishmaniasis and pulmonary aspergillosis infection, J. Control. Release 160 (2012) 685–691. http://dx.doi.org/10.1016/j.jconrel.2012.04.004.
[30] N. Uyanik, C. Erbil, Monomer reactivity ratios of itaconic acid and acrylamide copolymers determined by using potentiometric titration method, Eur. Polym. J. 36 (2000) 2651–2654.
[31] B.C. Hancock, M. Parks, What is the true solubility advantage for amorphous pharmaceuticals? Pharm. Res. 17 (2000) 397–404 (http://www.ncbi.nlm.nih.gov/pubmed/10870982).
[32] S. Clas, C. Dalton, B. Hancock, Differential scanning calorimetry: applications in drug development, Pharm. Sci. Technol. Today 2 (1999) 311–320 (http://www.ncbi.nlm.nih.gov/pubmed/10441275).
[33] The United States Pharmacopeial Convention, United States Pharmacopeia and National Formulary, Rockville, MD, 2007. (USP 30–NF 25).
[34] H.-C. Wang, W. John, Particle density correction for the aerodynamic particle sizer, Aerosol Sci. Technol. 6 (1987) 191–198. http://dx.doi.org/10.1080/02786828708959132.
[35] J.X. Zhang, X.J. Li, L.Y. Qiu, X.H. Li, M.Q. Yan, Yi Jin, et al., Indomethacin-loaded polymeric nanocarriers based on amphiphilic polyphosphazenes with poly (N-isopropylacrylamide) and ethyl tryptophan as side groups: preparation, in vitro and in vivo evaluation, J. Control. Release 116 (2006) 322–329. http://dx.doi.org/10.1016/j.jconrel.2006.09.013.
[36] R.H. Manzo, A.F. Jimenez-Kairuz, M.E. Olivera, F. Alovero, M.V. Ramirez Rigo, Thermodynamic and rheological properties of polyelectrolyte systems, Polyelectrolytes, Thermodynamics and Rheology, Springer International Publishing Switzerland, 2014, pp. 215–244.
[37] A. Jimenez-Kairuz, M. Ramirez Rigo, D. Quinteros, A. Vilches, M. Olivera, F. Alovero, et al., Recientes contribuciones sobre la utilización de polielectrolitos en sistemas portadores de fármacos. Parte I: Dispersiones Acuosas, Rev. Farm. 150 (2008) 11–25.
[38] U. Gupta, H.B. Agashe, N.K. Jain, Polypropylene imine dendrimer mediated solubility enhancement: effect of pH and functional groups of hydrophobes, J. Pharm. Pharm. Sci. 10 (2007) 358–367 (http://www.ncbi.nlm.nih.gov/pubmed/17727799).
[39] R. Kolakovic, T. Laaksonen, L. Peltonen, A. Laukkanen, J. Hirvonen, Spray-dried nanofibrillar cellulose microparticles for sustained drug release, Int. J. Pharm. 430 (2012) 47–55. http://dx.doi.org/10.1016/j.ijpharm.2012.03.031.
[40] N.-H. Chun, I.-C. Wang, M.-J. Lee, Y.-T. Jung, S. Lee, W.-S. Kim, et al., Characteristics of indomethacin–saccharin (IMC–SAC) co-crystals prepared by an anti-solvent crystallization process, Eur. J. Pharm. Biopharm. 85 (2013) 854–861.
[41] W. Limwikrant, M. Osada, K. Higashi, Y. Tozuka, K. Moribe, K. Yamamoto, Unique indomethacin nanoparticles formation by cogrinding with dextrin under defined moisture conditions, Powder Technol. 221 (2012) 213–219. http://dx.doi.org/10.1016/j.powtec.2012.01.004.
[42] E.C. Frascareli, V.M. Silva, R.V. Tonon, M.D. Hubinger, Effect of process conditions on the microencapsulation of coffee oil by spray drying, Food Bioprod. Process. 90 (2012) 413–424. http://dx.doi.org/10.1016/j.fbp.2011.12.002.
[43] M. Rusu, M. Olea, D. Rusu, Kinetic study of the indomethacin synthesis and thermal decomposition reactions, J. Pharm. Biomed. Anal. 24 (2000) 19–24.
[44] A. Mauerer, G. Lee, Changes in the amide I FT-IR bands of poly-L-lysine on spray-drying from alpha-helix, beta-sheet or random coil conformations, Eur. J. Pharm. Biopharm. 62 (2006) 131–142.
[45] L. Gallo, J.M. Llabot, D. Allemandi, V. Bucalá, J. Piña, Influence of spray-drying operating conditions on *Rhamnus purshiana* (Cáscara sagrada) extract powder physical properties, Powder Technol. 208 (2011) 205–214. http://dx.doi.org/10.1016/j.powtec.2010.12.021.

[46] N.R. Rabbani, P.C. Seville, The influence of formulation components on the aerosolisation properties of spray-dried powders, J. Control. Release 110 (2005) 130–140. http://dx.doi.org/10.1016/j.jconrel.2005.09.004.
[47] F. Sansone, T. Mencherini, P. Picerno, M. D'Amore, R.P. Aquino, M.R. Lauro, Maltodextrin/pectin microparticles by spray drying as carrier for nutraceutical extracts, J. Food Eng. 105 (2011) 468–476.
[48] C.J. Strachan, T. Rades, K.C. Gordon, A theoretical and spectroscopic study of gamma-crystalline and amorphous indometacin, J. Pharm. Pharmacol. 59 (2007) 261–269. http://dx.doi.org/10.1211/jpp.59.2.0012.
[49] R.T. Conley, Infrared Spectroscopy, 2nd ed., 1972. (Alhambra, Spain).
[50] H. Garcia, A.S. Barros, C. Gonçalves, F.M. Gama, A.M. Gil, Characterization of dextrin hydrogels by FTIR spectroscopy and solid state NMR spectroscopy, Eur. Polym. J. 44 (2008) 2318–2329. http://dx.doi.org/10.1016/j.eurpolymj.2008.05.013.
[51] P. Karmwar, K. Graeser, K.C. Gordon, C.J. Strachan, T. Rades, Investigation of properties and recrystallisation behaviour of amorphous indomethacin samples prepared by different methods, Int. J. Pharm. 417 (2011) 94–100. http://dx.doi.org/10.1016/j.ijpharm.2010.12.019.
[52] A.V. Ewing, G.S. Clarke, S.G. Kazarian, Stability of indomethacin with relevance to the release from amorphous solid dispersions studied with ATR-FTIR spectroscopic imaging, Eur. J. Pharm. Sci. 60 (2014) 64–71. http://dx.doi.org/10.1016/j.ejps.2014.05.001.
[53] T.J. Kistenmacher, R.E. Marsh, Crystal and molecular structure of an antiinflammatory agent, indomethacin, 1-(p-chlorobenzoyl)-5-methoxy-2-methylindole-3-acetAicc id, J. Am. Chem. Soc. 94 (1972) 1340–1345.
[54] Y. Shimada, S. Goto, H. Uchiro, H. Hirabayashi, K. Yamaguchi, K. Hirota, et al., Features of heat-induced amorphous complex between indomethacin and lidocaine, Colloids Surf. B: Biointerfaces 102 (2013) 590–596. http://dx.doi.org/10.1016/j.colsurfb.2012.08.060.
[55] K. Maiti, K. Mukherjee, A. Gantait, B.P. Saha, P.K. Mukherjee, Curcumin–phospholipid complex: preparation, therapeutic evaluation and pharmacokinetic study in rats, Int. J. Pharm. 330 (2007) 155–163. http://dx.doi.org/10.1016/j.ijpharm.2006.09.025.
[56] N. Bandi, W. Wei, C.B. Roberts, L.P. Kotra, U.B. Kompella, Preparation of budesonide- and indomethacin-hydroxypropyl-beta-cyclodextrin (HPBCD) complexes using a single-step, organic-solvent-free supercritical fluid process, Eur. J. Pharm. Sci. 23 (2004) 159–168. http://dx.doi.org/10.1016/j.ejps.2004.06.007.
[57] M.J. Donovan, H.D.C. Smyth, Influence of size and surface roughness of large lactose carrier particles in dry powder inhaler formulations, Int. J. Pharm. 402 (2010) 1–9. http://dx.doi.org/10.1016/j.ijpharm.2010.08.045.
[58] I.M. El-Sherbiny, H.D.C. Smyth, Controlled release pulmonary administration of curcumin using swellable biocompatible microparticles, Mol. Pharm. 9 (2012) 269–280. http://dx.doi.org/10.1021/mp200351y.